The Abdus Salam International Centre for Theoretical Physics

United Nations Educational, Scientific and Cultural Organization
IAEA International Atomic Energy Agency

2058-S-6

Pseudochaos and Stable-Chaos in Statistical Mechanics and Quantum Physics

21 - 25 September 2009

Quantum chaos and unpredictability in quantum systems

U. SMILANSKY
Weizmann Institute of Science
Rehovot
Israel

Trieste September 2009

Quantum Chaos and **Unpredictability** in Quantum Systems

Organizers, is this in earnest ?

1. The importance of being **quantal**
2. The importance of being **irrational.**
3. The importance of being **well-connected**

Quantum Scrambling

1. The importance of being quantal

The Quantum chaos paradigm: Level statistics

Nearest neigbour spectral distribution

$s_n = \frac{\lambda_n - \lambda_{n-1}}{\text{mean spacing}}$; $P(s) = \frac{1}{K} \sum_{k=N+1}^{N+K} \delta(s - s_k)$

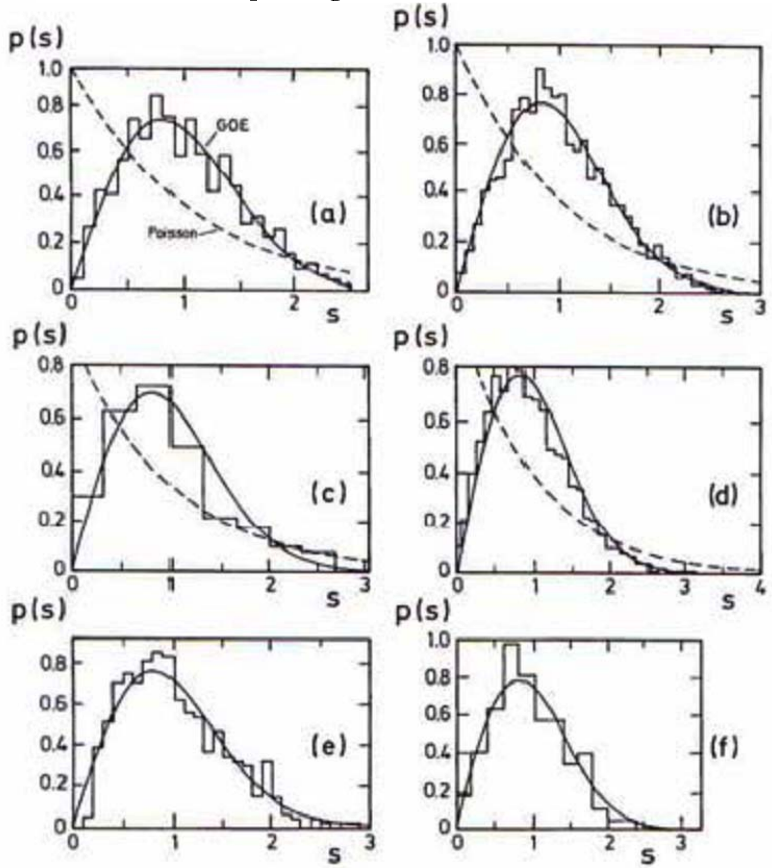

Fig. 1.4. Level spacing distributions for (a) the Sinai billiard[7], (b) a hydrogen atom in a strong magnetic field [20], (c) an NO_2 molecule [16], (d) a vibrating quartz block shaped like a three dimensional Sinai billiard [21], (e) the microwave spectrum of a three-dimensional chaotic cavity [22], (f) a vibrating elastic disc shaped like a quarter stadium [23]. Courtesy of Stöckmann

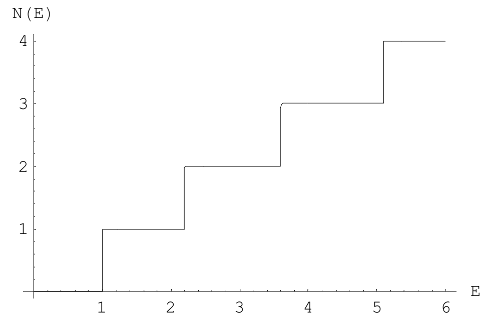

$$N(E) = \frac{\mathcal{A}}{4\pi} E - \frac{\mathcal{L}}{4\pi} E^{\frac{1}{2}} + \mathcal{O}(1) + \sum_p a_p \cos(l_p\, E^{\frac{1}{2}} + \phi_p)$$

$\mathcal{A}$: The area of the drum.

$\mathcal{L}$: The length of its circumference.

p : periodic orbit of length l_p.

a_p : "stability amplitudes".

Key-word: interference

Can one hear the shape of a drum?

Nature 177, 27 (1956)

A TEST OF A NEW TYPE OF STELLAR INTERFEROMETER ON SIRIUS

By R. HANBURY BROWN
Jodrell Bank Experimental Station, University of Manchester
AND
DR. R. Q. TWISS
Services Electronics Research Laboratory, Baldock

$$C_{1,2}(d) = \frac{\langle I_1 \ I_2 \rangle - \langle I_1 \rangle \langle I_2 \rangle}{\langle I_1 \rangle \langle I_2 \rangle}$$

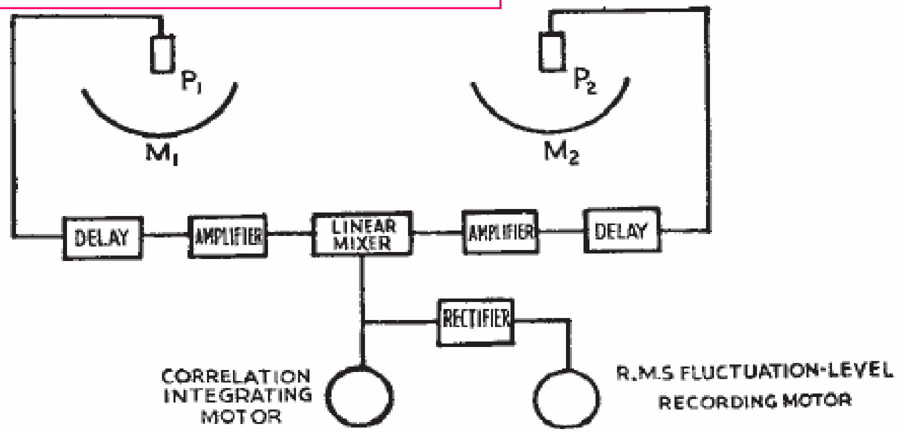

Fig. 1. Simplified diagram of the apparatus

$$C(\vec{d}\,) \sim \left| \int d^3 r \rho(\vec{r}\,) e^{i(\vec{k}_1 - \vec{k}_2)\cdot\vec{r}} \right|^2$$

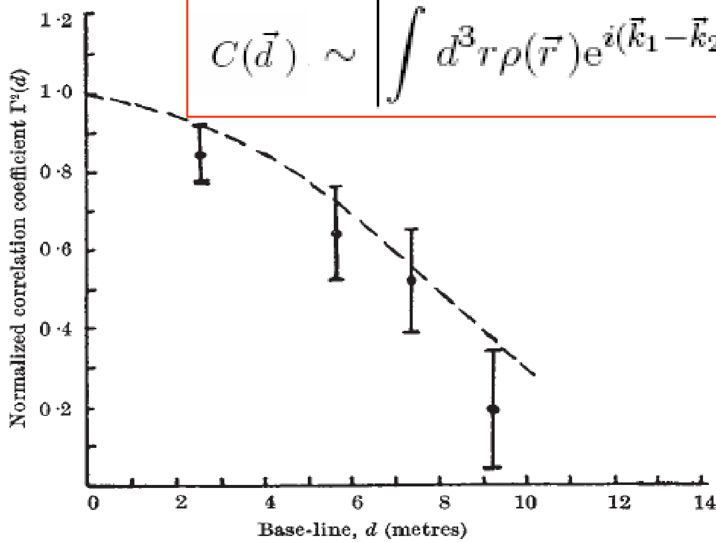

Fig. 2. Comparison between the values of the normalized correlation coefficient $\Gamma^2(d)$ observed from Sirius and the theoretical values for a star of angular diameter 0·0063″. The errors shown are the probable errors of the observations

VOLUME 10, NUMBER 3 PHYSICAL REVIEW LETTERS 1 FEBRUARY 1963

PHOTON CORRELATIONS*

Roy J. Glauber
Lyman Laboratory, Harvard University, Cambridge, Massachusetts

It is easily shown that coherent states of the field lead to no photoionization correlations at all.

Chaotic scattering version of the Hanbury-BrownTwiss experiment

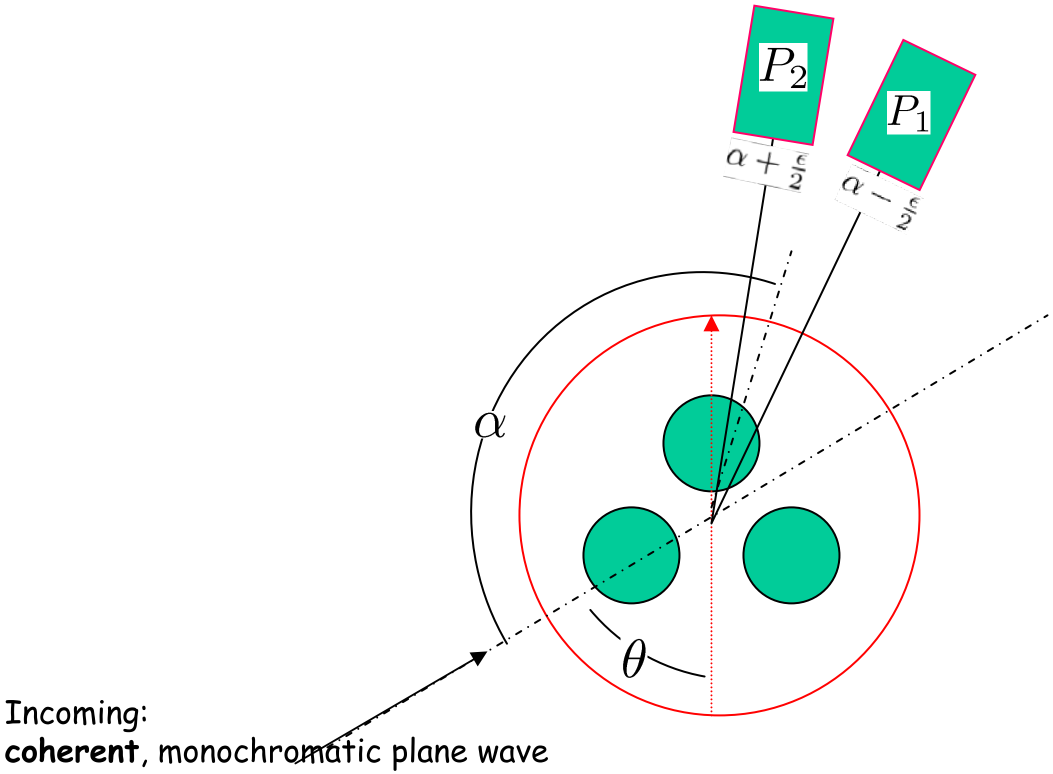

Measure: Intensity (not amplitude!) correlations at the detectors
As a function of their angular distance average over the table angle θ

$$\langle \cdot \rangle \equiv \int_0^{2\pi} \frac{\mathrm{d}\theta}{2\pi} (\cdot)$$

$$C_{1,2}(\epsilon) = \left\langle \frac{I(\alpha + \epsilon/2;\theta) I(\alpha - \epsilon/2;\theta) - \langle I(\alpha) \rangle^2}{\langle I(\alpha) \rangle^2} \right\rangle$$

$$f(\theta,\theta+\alpha)=\sum_p a_p(\theta,\theta+\alpha)\mathrm{e}^{ikS_p(\theta,\theta+\alpha)}$$

p: classical scattering trajectory $\theta\to\theta+\alpha$
a_p semiclassical amplitude associated with p

$$\langle I(\alpha)\rangle=\int_0^{2\pi}\frac{\mathrm{d}\theta}{2\pi}|f(\theta,\theta+\alpha)|^2=\sum_{p,q}\int_0^{2\pi}\frac{\mathrm{d}\theta}{2\pi}a_p a_q^\star \mathrm{e}^{ik(S_p-S_q)}$$

For chaotic trajectories

$$\int_0^{2\pi}\frac{\mathrm{d}\theta}{2\pi}\mathrm{e}^{ik(S_p-S_q)}\approx\delta_{p,q}\quad (\text{“diagonal approximation”})$$

$$\langle I(\alpha)\rangle\approx\sum_p|a_p|^2 \quad p: \text{ class. traj. deflected by an angle } \alpha$$

$$\left\langle I(\alpha+\frac{\epsilon}{2})I(\alpha-\frac{\epsilon}{2})\right\rangle=\sum_{p,q,r,s}\int_0^{2\pi}\frac{\mathrm{d}\theta}{2\pi}a_p a_q^\star a_r a_s^\star \mathrm{e}^{ik(S_p-S_q+S_r-S_s)}$$

p,q: classical scattering trajectory $\theta\to\theta+\alpha+\frac{\epsilon}{2}$
r,s: classical scattering trajectory $\theta\to\theta+\alpha-\frac{\epsilon}{2}$

$$S_p(\theta,\theta+\alpha\pm\frac{\epsilon}{2})\approx S_p(\theta,\theta+\alpha)\pm\frac{\epsilon}{2}\,l_p^{(f)}$$

$$\left\langle I(\alpha+\frac{\epsilon}{2})\langle I(\alpha-\frac{\epsilon}{2})\right\rangle = \sum_{p,q,r,s}\int_0^{2\pi}\frac{\mathrm{d}\theta}{2\pi}a_p a_q^\star a_r a_s^\star \mathrm{e}^{ik(S_p-S_q+S_r-S_s)}$$

p,q: classical scattering trajectory $\theta \to \theta+\alpha+\frac{\epsilon}{2}$
r,s: classical scattering trajectory $\theta \to \theta+\alpha-\frac{\epsilon}{2}$

$$S_p(\theta,\theta+\alpha\pm\frac{\epsilon}{2}) \approx \ S_p(\theta,\theta+\alpha)\pm\frac{\epsilon}{2}\ l_p^{(f)}$$

$$\left\langle I(\alpha+\frac{\epsilon}{2})\langle I(\alpha-\frac{\epsilon}{2})\right\rangle \approx \sum_{p,q,r,s} a_p a_q^\star a_r a_s^\star(\delta_{p,q}\delta_{r,s}+\delta_{p,s}\delta_{q,r}\mathrm{e}^{ik(l_p^{(f)}-l_q^{(f)})\epsilon}\ )$$

p,q : Calssical trajectories which deflect by an angle α
$l_p^{(f)}$ outgoing angular momentom on the trajectory p

$$\approx \langle I(\alpha)\rangle^2\left(1+\left|\sum_p |a_p|^2\mathrm{e}^{ikl_p^{(f)}\epsilon}\right|^2\right) \approx \langle I(\alpha)\rangle^2\left(1+\left|\int \mathrm{d}l\rho(l)\ \mathrm{e}^{ikl\epsilon}\right|^2\right)$$

$\rho(l)$: probability that a class. traj. emerges with an angular momentum l
supported on an interval of length kD, D : diameter of the scatterer.

$$C_{1,2}(\epsilon=0)=1.$$

Nodal domains

1.Separable (integrable)
Checker board strucrure

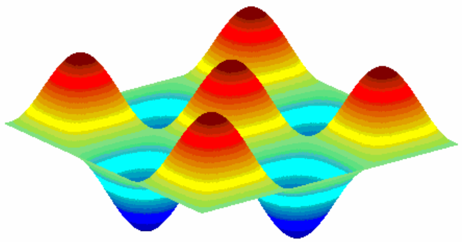

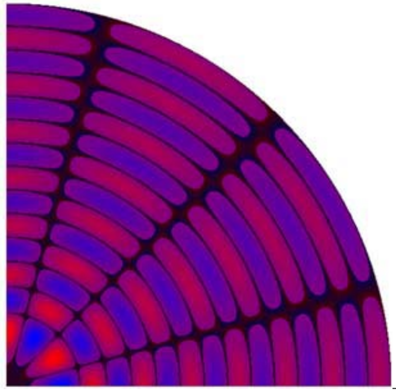

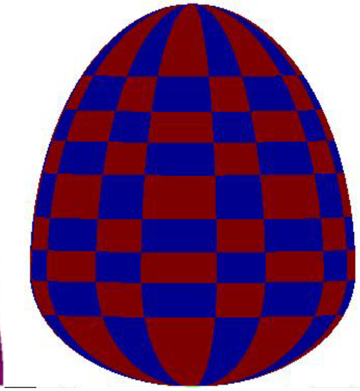

2. Non-separable (Integrable)

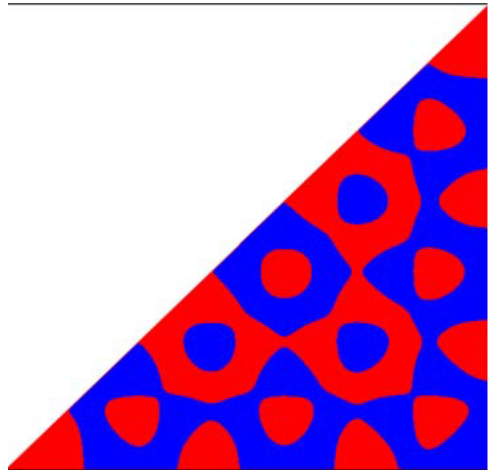

3. "Chaotic"

Stadium

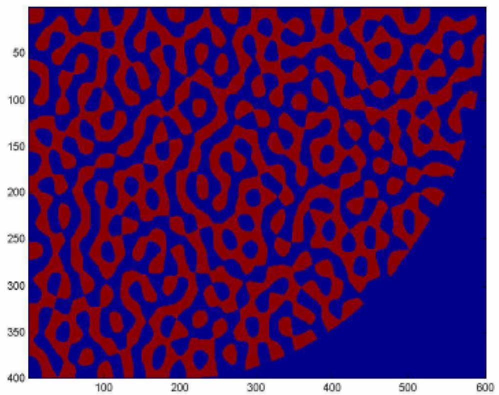

Africa

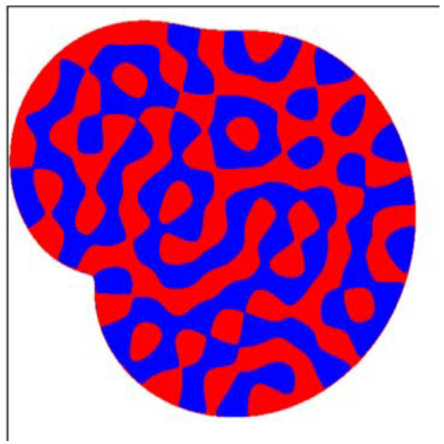

Sinai

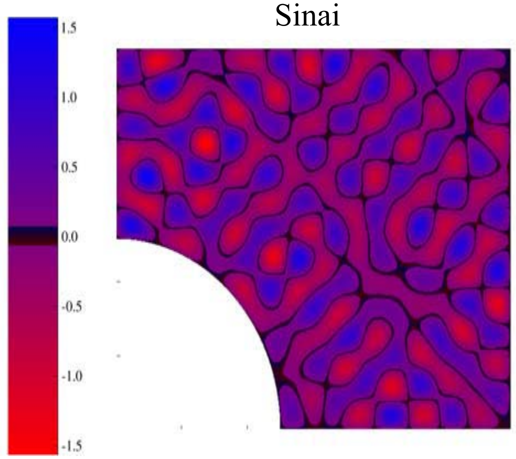

The transition from an integrable to a chaotic domain

Random waves

Random Gaussian fields $\psi(\mathbf{r}) \; : \; \mathbf{r} \in \Omega \in R^2 \rightarrow R$

$$\Delta\psi(\mathbf{r}) = k^2\psi(\mathbf{r})$$

$$\langle \psi(\mathbf{r})\psi(\mathbf{r}')\rangle \quad = \quad J_0(k|\,\mathbf{r} - \mathbf{r}'|)$$

Realization:

$$\psi(\mathbf{r}) = \sum_{l=0}^{L} J_l(kr)(a_l \sin l\theta + b_l \cos l\theta) \;,\; L = k|\Omega|$$

a_l, b_l independent identically distributed Gaussian variables.

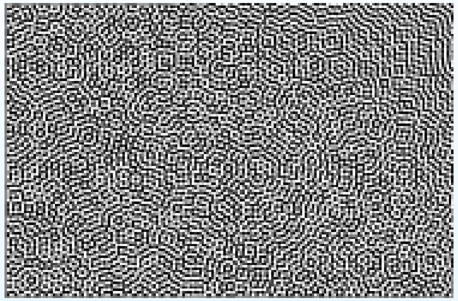

Nodal domains of stadium with $E = 10092.029$

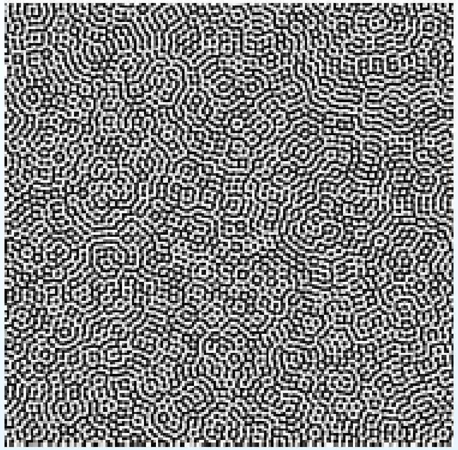

Gaussian random wave function with $k = 100$

Random Gaussian fields $\psi(\omega) \; : \; \omega \in S^2 \rightarrow R$

$$\Delta\psi(\omega) = l(l+1)\psi(\omega)$$

$$\langle \psi(\omega)\psi(\omega')\rangle = P_l(|\omega - \omega'|)$$

Realization:

$$\psi(\omega) = \sum_{m=-l}^{l} a_m Y_l^{(m)}(\omega) \;,\; a_{-m} = (-1)^m a_m^{\star}$$

$Re(a_m), Im(a_m)$ independent identically distributed Gaussian variables.

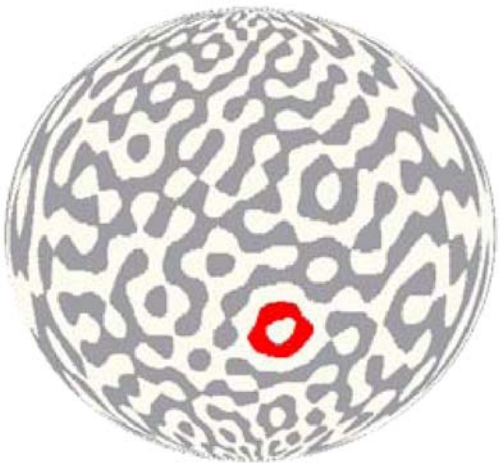

Random waves on the sphere

M. Berry Conjecture (1977) : The statistical properties of wave functions of chaotic billiards are faithfully described by the random wave model at the appropriate wave-number range.

The network on various scales:

The intersection-points of the nodal set with a reference line.

Amit Aronovitch and Uzy Smilansky
The statistics of the points where nodal lines intersect a reference curve.
J. Phys. A: Math. Theor. **40** 97439770 (2007)

The intersections are considered as a point process and studied statistically

Intersections in the bulk

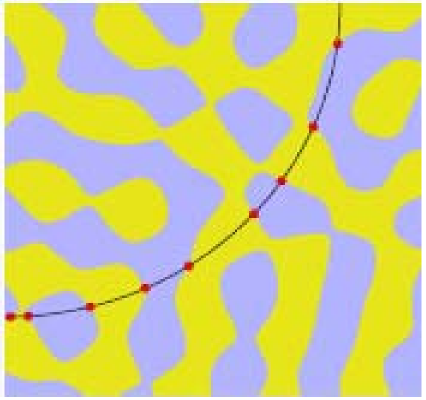

Intersections with the boundary

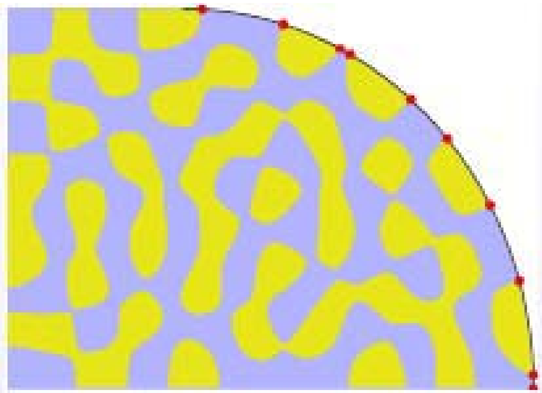

Short range statistics

Nearest spacing distribution:

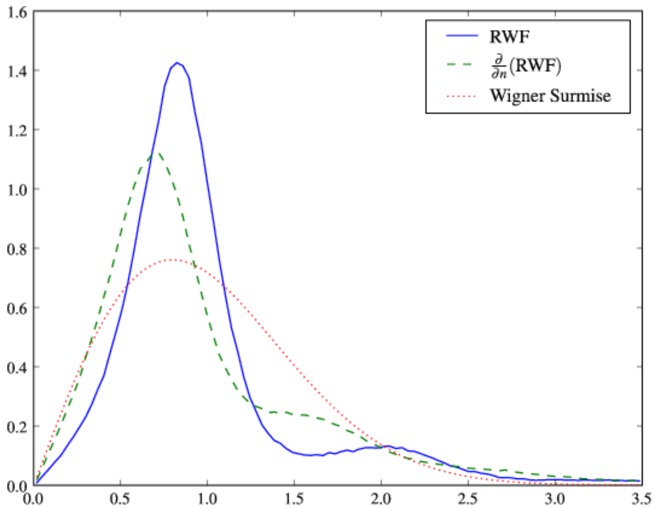

Long range correlations

The number variance : Let δ be the mean distance between successive intersections. Denote by $N(x)$ the number of intersections in an interval of length x.

$$var(n) = \left\langle (N(\delta \cdot n) - n)^2 \right\rangle \quad .$$

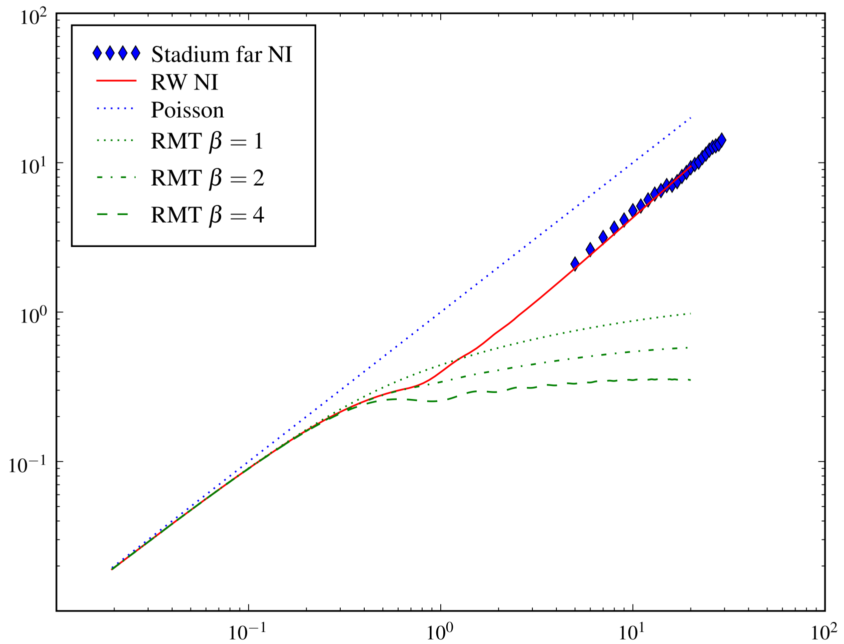

$$var(n) \approx n \log n \text{ for } \; n \to \infty$$

Compare: Poisson $var(n) \approx n$, RMT $var(n) \approx \log n$

Nodal domains and percolation theory

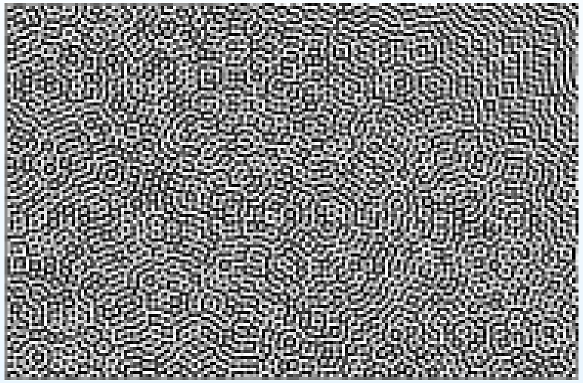

Nodal domains of stadium with $E = 10092.029$

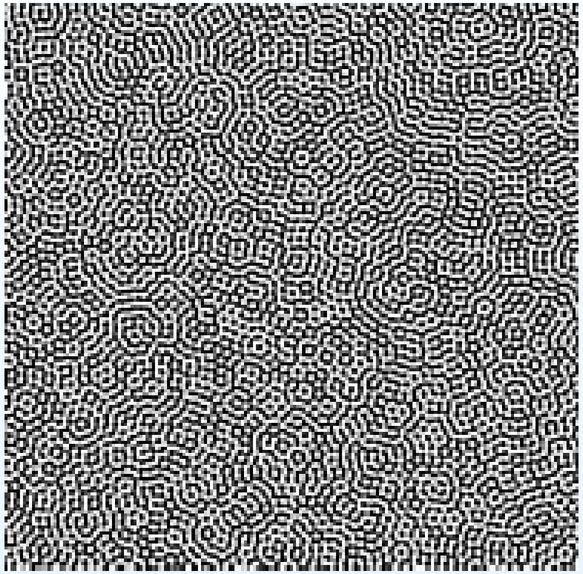

Gaussian random wave

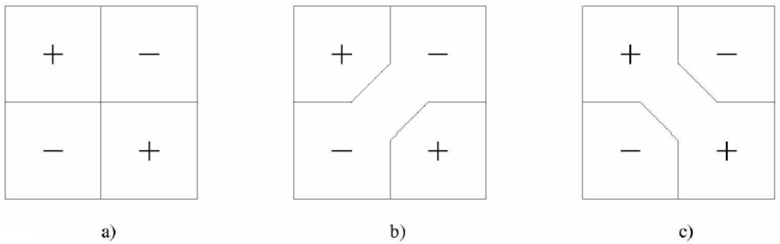

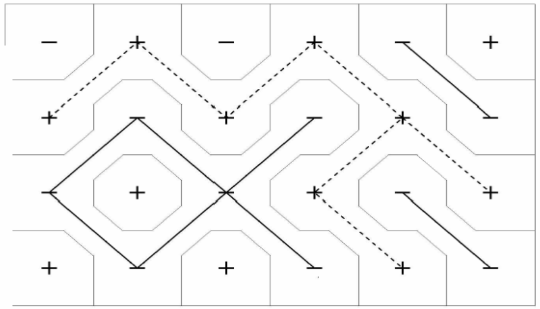

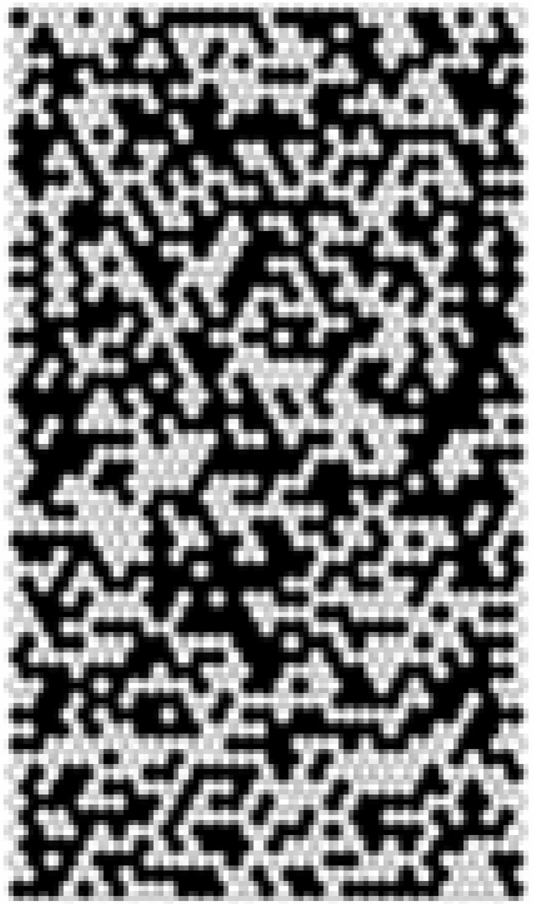

Nodal domains distribution.

E. Bogomolny and C. Schmit, Phys Rev Lett. **88**, 114102 (2002).

Percolation theory:

$$\langle \nu_n \rangle / n = \frac{3\sqrt{3}-5}{\pi} = 0.0624 \quad << \text{Pleijel's bound.}$$
$$var(\nu_n)/n = \frac{1}{\pi}(\frac{18}{\pi} + 4\sqrt{3} - \frac{25}{2}) = .0502$$

Predictions of percolation theory, comparison with the random waves model

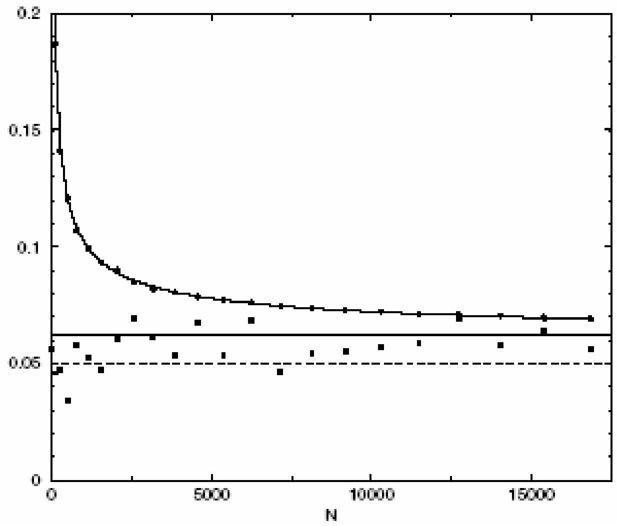

FIG. 4. Mean values of the nodal domains (dots) and their variances (squares) for random functions divided by N versus N. The solid and dashed horizontal lines represent theoretical asymptotic values (13) and (14), respectively.

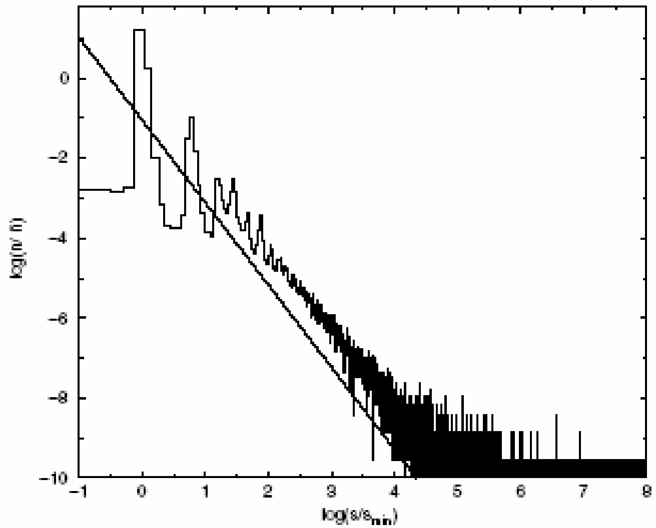

FIG. 5. Distribution of nodal domain areas. The solid line has the slope $\tau = 187/91$ predicted by the percolation theory.

And with a microwave experiment

PHYSICAL REVIEW E 70, 056209 (2004)

Experimental investigation of nodal domains in the chaotic microwave rough billiard

Nazar Savytskyy, Oleh Hul, and Leszek Sirko
Institute of Physics, Polish Academy of Sciences, Aleja Lotników 32/46, 02-668 Warszawa, Poland

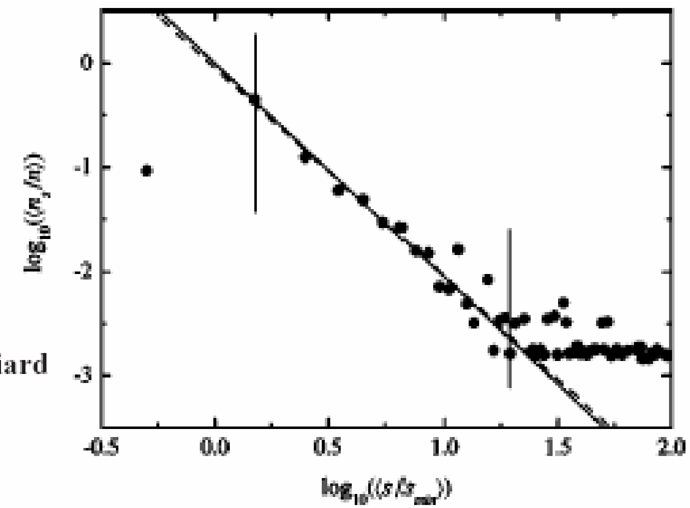

FIG. 7. Distribution of nodal domain areas. Full line shows the prediction of percolation theory $\log_{10}(\langle n_s/n\rangle) = -\frac{187}{91}\log_{10}(\langle s/s_{min}\rangle)$.

SLE: A theory which provides a uniform description
of conformally invariant self avoiding random lines in 2d

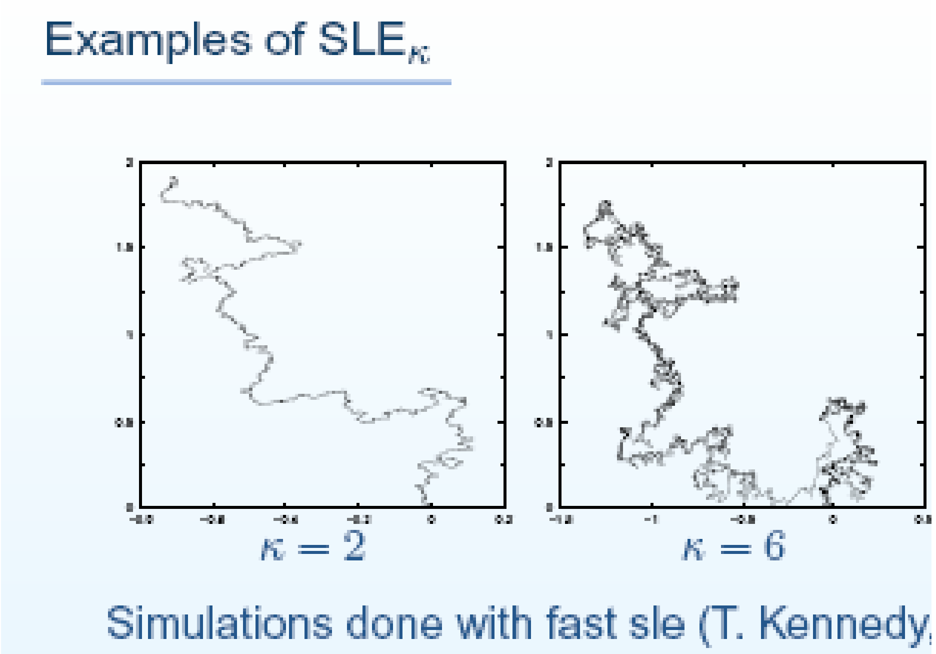

k=2 : Random walk

k=6 : Critical percolation

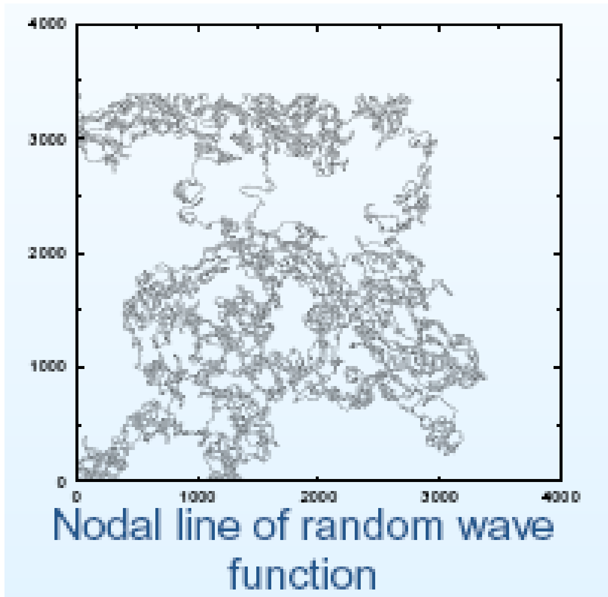

(Bogomolny *et al*, Keating *et al.*)

Can one count the shape of a drum?

2. The importance of being irrational

PHYSICAL REVIEW A VOLUME 29, NUMBER 4 APRIL 1984

Quantum dynamics of a nonintegrable system

D. R. Grempel* and R. E. Prange†
Department of Physics and Center for Theoretical Physics, University of Maryland, College Park, Maryland 20742

Shmuel Fishman
Department of Physics, Israel Institute of Technology (Technion), 32000 Haifa, Israel
(Received 11 July 1983)

$$T_m u_m + \sum_{r\,(\neq 0)} W_r u_{m+r} = E u_m$$

with

$$T_m = \tan\left[\frac{E_m}{2}\right] = \tan\left[\frac{\omega - K(m)}{2}\right] \qquad K(m) = \frac{\tau}{2} m^2$$

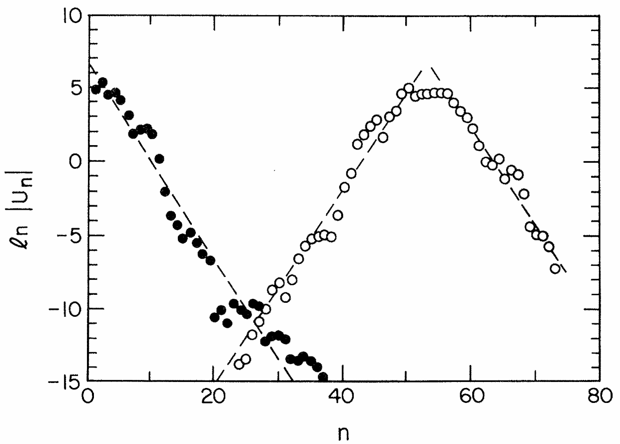

FIG. 4. Two quasienergy eigenstates for the same potential as in the previous plot. Quasienergies are $\omega = 2\pi j/2^{10}$ with $j = 323$ (solid circles) and $j = 621$ (open circles).

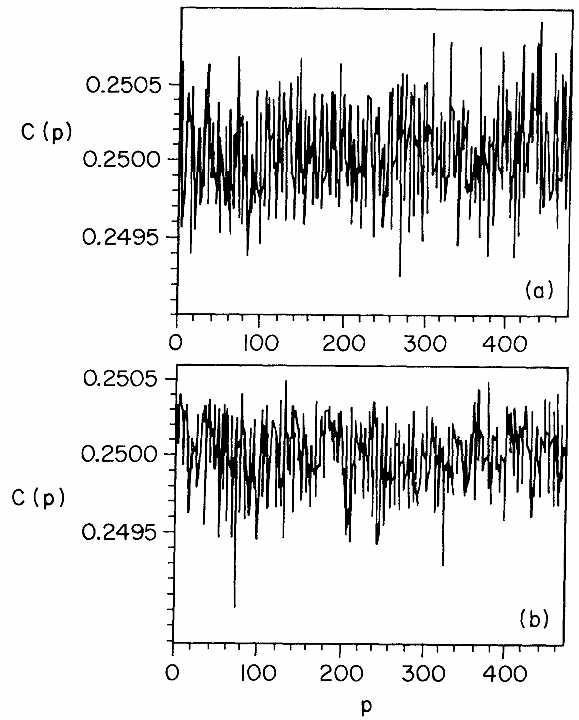

FIG. 1. Power spectrum of (a) the sequence $K_n = \sqrt{5} n^2$ (mod 1) and (b) a sequence of random numbers with uniform distribution in [0,1].

The Laplace operator on metric graphs ("Quantum Graphs")

A graph $\mathcal{G}$ is made of V **vertices** and B **bonds**.

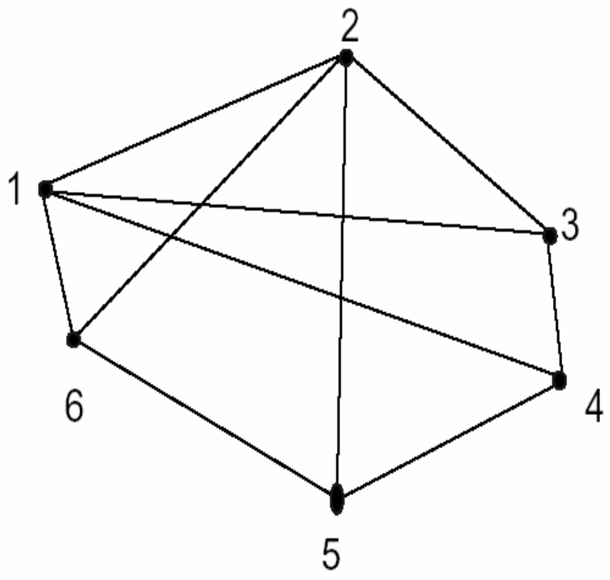

Figure 1. $V = 6$ graph.

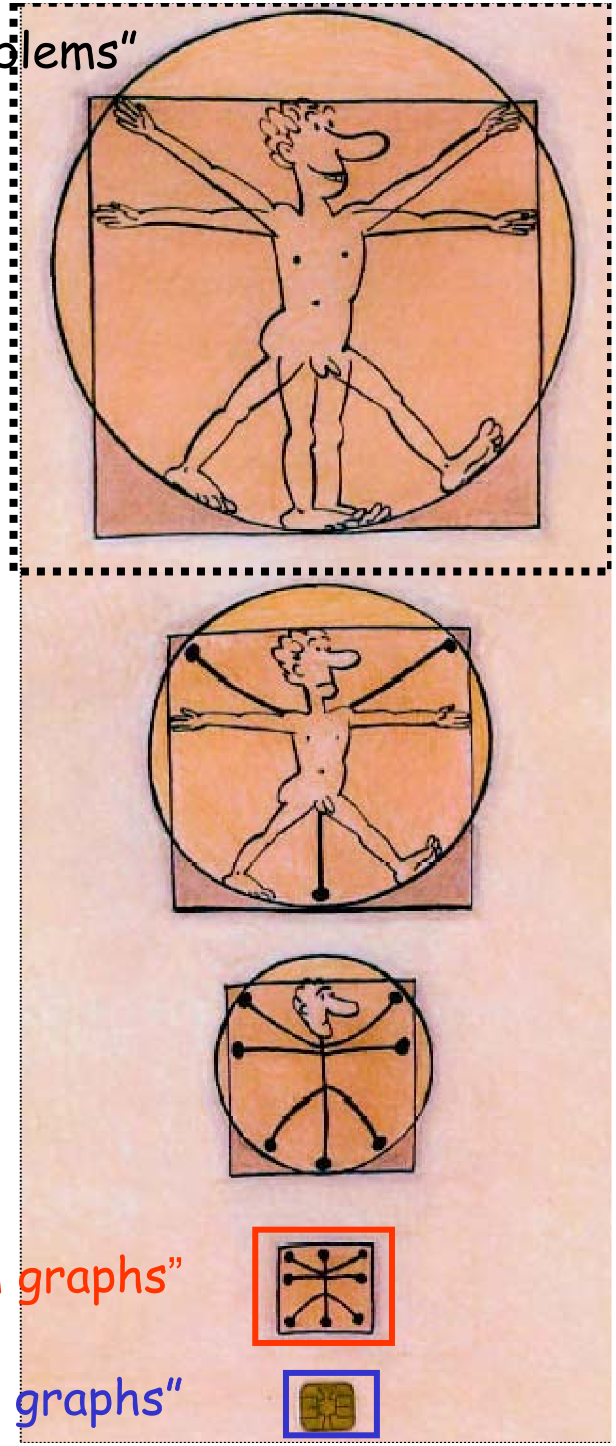

Connectivity matrix :

$C_{i,j}(\mathcal{G}) = \ \#$ bonds connecting i and j.

Simple graph: $C_{i,j} \in [0,1]$; $C_{i,i} = 0 \ \ \forall i \ , \ \ j$
(No parallel bonds, no loops).

Bond : $b \ = \ [i,j]$,

Directed bond : $d \ = \ (i,j)$, $\hat{d} \ = \ (j,i)$.

B: Total number of bonds $= \frac{1}{2} \sum_{i,j=1}^{V} C_{i,j}$

v_i: Valency of a vertex $= \sum_{j=1}^{V} C_{i,j}$

The Schroedinger operator on graphs:

1. The wave function

$$\Psi(x) = \psi_b(x_b) \text{ for } x \in b \ , \quad b = 1, \cdots, B$$

$\Psi(x)$ continuous at the verices,

$\psi_b(x_b)$ doubly differentiable in $(0, L_b)$

2. The wave equation

On each bond: $$\left(\frac{1}{i}\frac{\mathrm{d}}{\mathrm{d}x_b} - A_b\right)^2 \psi_b(x_b) = k^2 \psi_b(x_b)$$

3. The boundary conditions at the vertices i = 1,…V

Neumann : $$\sum_{b \in S^i} \left(\frac{1}{i}\frac{\mathrm{d}}{\mathrm{d}x_b} - A_b\right) \psi_b(x_b)\Big|_i = 0$$. Dirichlet : $$\psi_b(x_b)|_i = 0$$

The Schroedinger operator is self – adjoint
with real and non-negative discrete spectrum $\left\{k_n^2\right\}_{n=1}^{\infty}$

The **1st** surprising numerical evidence (Tsampikos Kottos, U.S., (1997))

$$I(s) = \int_0^s p(x)\mathrm{d}x$$

= cumulative level-spacing distribution

Only works when the bond-lengths are rationally independent.
For sufficiently well connected graphs
Spectral statistics -> RMT in the limit $B \to \infty$

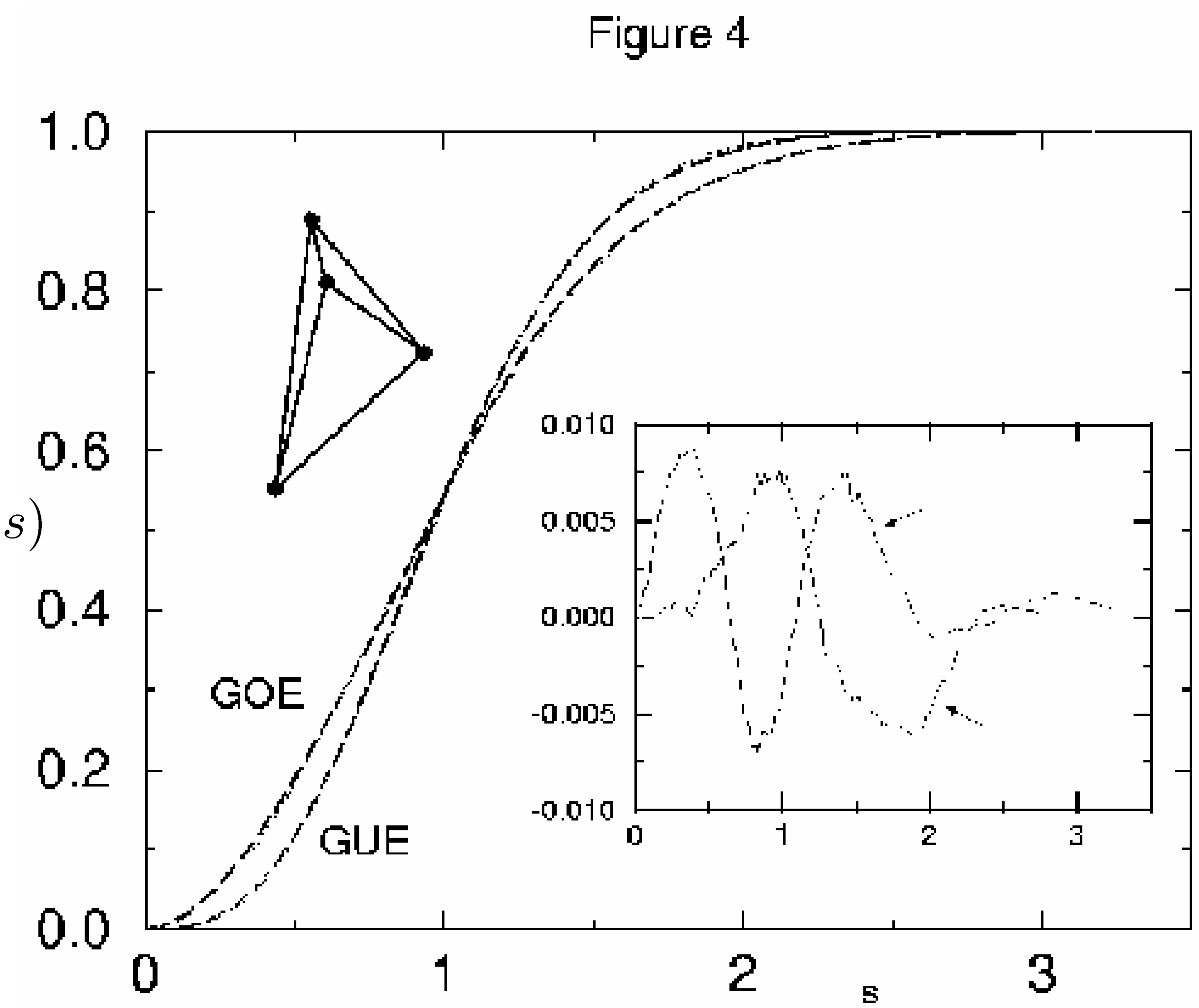

Figure 3. Integrated nearest neighbor distribution $I(s)$ for a fully connected $V = 4$ graph (Neumann boundary conditions), using the lowest 80,000 eigenvalues. Inset: the deviation from the exact GOE/GUE results;

The Secular equation

$$\zeta(k) \ = \ \det(I - U(k)) \ = \ 0.$$

$$U_{d',d}(k) = \mathrm{e}^{ikL_{d'}} \sigma_{d',d} \delta_{o(d'),t(d)}$$

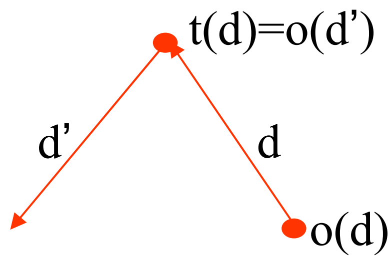

On the Distribution of the Values of Real Almost Periodic Functions

M. Kac, E. R. van Kampen, Aurel Wintner

American Journal of Mathematics, Vol. 61, (1939), pp. 985-99

$\zeta(k)$ is quasi-periodic in k through the phases $\phi_b = kL_b$.
Ergodicity:

$$\frac{1}{K}\int_0^K F(\zeta(k))\mathrm{d}k \ \rightarrow \ \frac{1}{(2\pi)^B}\int_0^{2\pi} \mathrm{d}\phi_1 \cdots \int_0^{2\pi} \mathrm{d}\phi_B F(\zeta(\phi_1, \cdots, \phi_B))$$

Which is true only if the bond lengths are rationally independent

Can on hear the shape of a graph?

3. The importance of being **well-connected**

or

Quantum chaos on discrete graphs

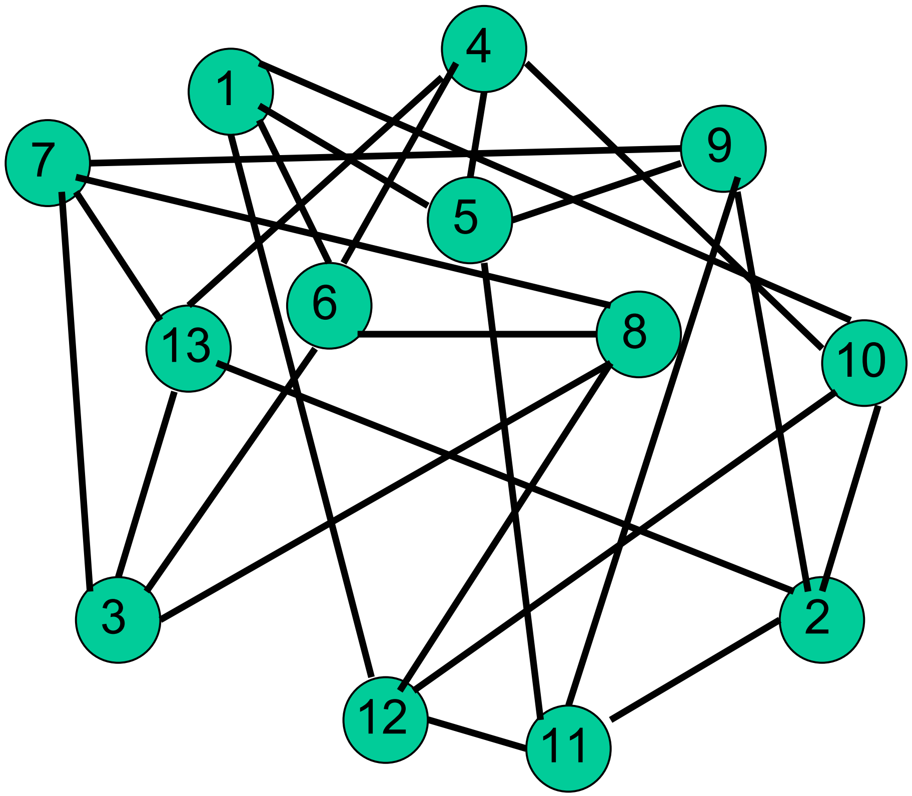

A short reminder

A graph $\mathcal{G}$ is a set $\mathcal{V}$ of vertices connected by a set $\mathcal{E}$ of edges.
The number of vertices : $V = |\mathcal{V}|$
The number of edges : $E = |\mathcal{E}|$.

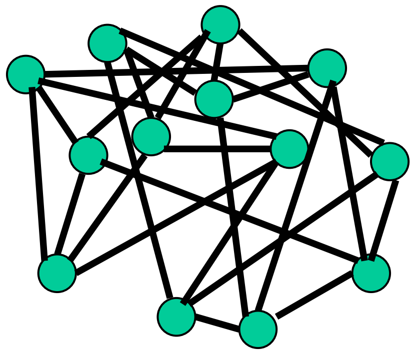

The $V \times V$ *adjacency* (*connectivity*) matrix A:
$A_{i,j} = 1$ if the vertices i, j are connected and 0 otherwise, $A_{i,i} = 0$.

degree d_i (*valency*) : $\sharp$ { edges emanating from the vertex}, $d_i = \sum_{j=1}^{V} A_{i,j}$

d**-regular graph** :
$d_i = d \ \ \forall\ i : 1 \le i \le V$,
$E = Vd/2$ Hence Vd is even.

d-regular graphs :
Expanders, Ramanujan

$\mathcal{G}_{V,d}$. The ensemble of all the d regular graphs with V vertices .

For fixed d and $V \to \infty$: $|\mathcal{G}_{V,d}| \approx \sqrt{2} e^{\frac{1-d^2}{4}} \left(\frac{d^d V^d}{e^d (d!)^2} \right)^{\frac{V}{2}}$

$\langle \cdots \rangle_{\mathcal{G}}$: Ensemble average taken with uniform probability distribution.

The spectrum and spectral statistics

The discrete Laplacian for d-regular graphs:

$$(L\mathbf{f})_i = -\sum_{j\sim i}(f_j - f_i) \;\Rightarrow\; L = -A + d\ I^{(V)}$$

Since L differes from the adjacency matrix A by a constant diagonal matrix, $\Rightarrow$ we study the spectrum of A : $\sigma(\mathcal{G}) = \lambda_0 (= d) \geq \lambda_1 \geq, \cdots, \geq \lambda_{V-1}$.

$$\rho(\lambda) = \frac{1}{V-1}\sum_{k=1}^{V-1}\delta(\lambda - \lambda_k)$$

The mean spectral density for d regular graphs, $(V \to \infty\ ,\ d = const)$

Kesten MacKay limit distribution: (Supported in $|\lambda| < 2\sqrt{d-1}$):

$$\rho_{KM}(\lambda) = \lim_{V\to\infty}\frac{1}{V-1}\left\langle \sum_{k=1}^{V-1}\delta(\lambda - \lambda_k)\right\rangle_{\mathcal{G}} = \frac{d}{2\pi}\frac{\sqrt{4(d-1)-\lambda^2}}{d^2-\lambda^2}$$

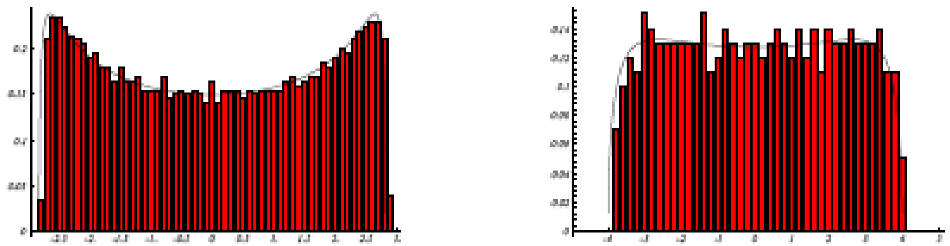

(a) Cubic graph on 2000 vertices. (b) 5-valent graph on 500 vertices.

Figure 1. Eigenvalue distributions of random graphs *vs* McKay's law

EIGENVALUE SPACINGS FOR REGULAR GRAPHS

DMITRY JAKOBSON, STEPHEN D. MILLER,
IGOR RIVIN AND ZEÉV RUDNICK

Unfolding the spectrum with the Kesten-McKay density

$$s_j = \mathcal{N}_{KM}(\lambda_j) \quad ; \quad \frac{\mathrm{d}\mathcal{N}_{KM}}{\mathrm{d}\lambda} = \rho_{KM}(\lambda)$$

$\mathcal{N}_{KM}$: The mean spectral counting function.

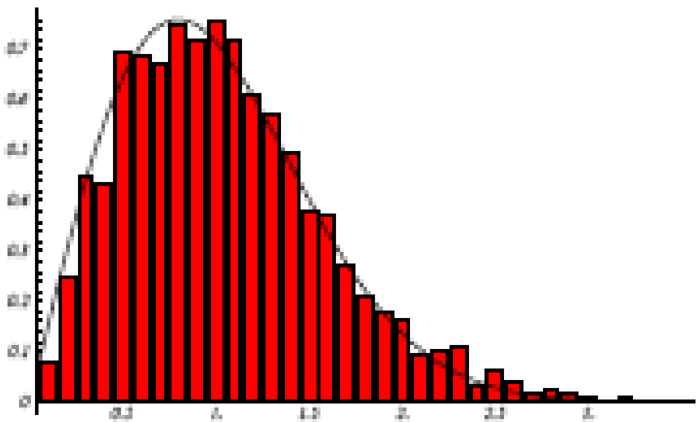

Figure 2. Level spacing distribution of a cubic graph on 2000 vertices *vs* GOE

The "Magnetic" Adjacency Matrix:

$$A_{i,j}^{(M)} = A_{i,j} \mathrm{e}^{i\phi_{i,j}} \quad ; \quad \phi_{j,i} = -\phi_{i,j}$$

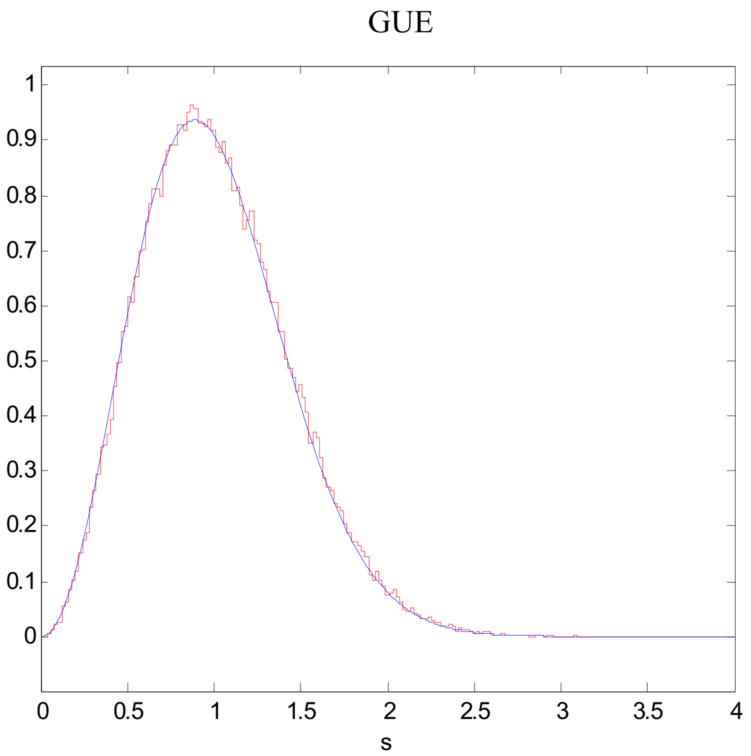

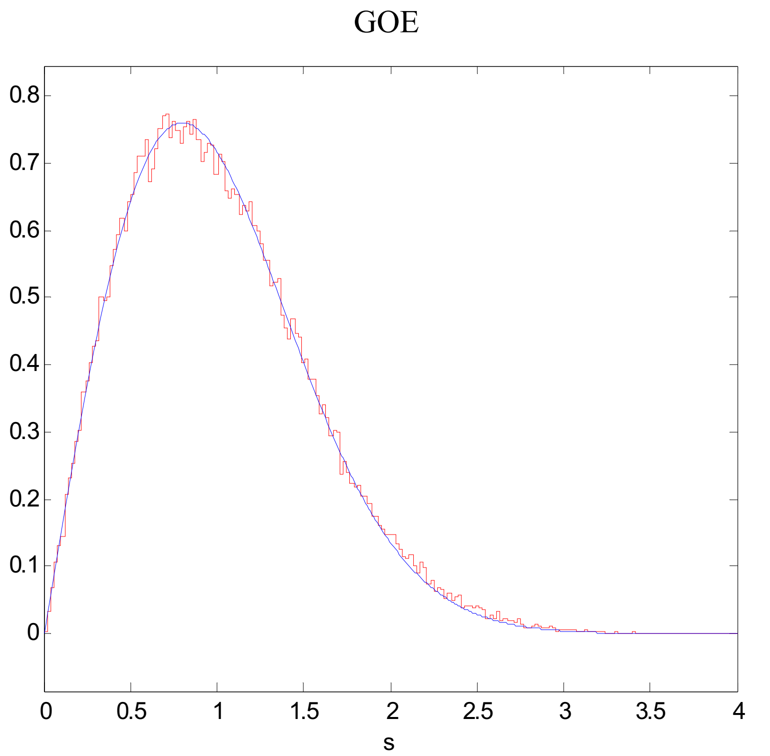

Spectral 2-points correlations:

$$\theta_j = 2\pi \frac{\mathcal{N}_{MK}(\lambda_j)}{V-1} \qquad \text{(mapping the spectrum on the unit circle)}$$

$$K(\tau) = \frac{1}{V-1} \left\langle \sum_{i,j=1}^{V-1} \cos(\theta_i - \theta_j)t \right\rangle , \quad \text{and} \quad t = (V-1)\tau$$

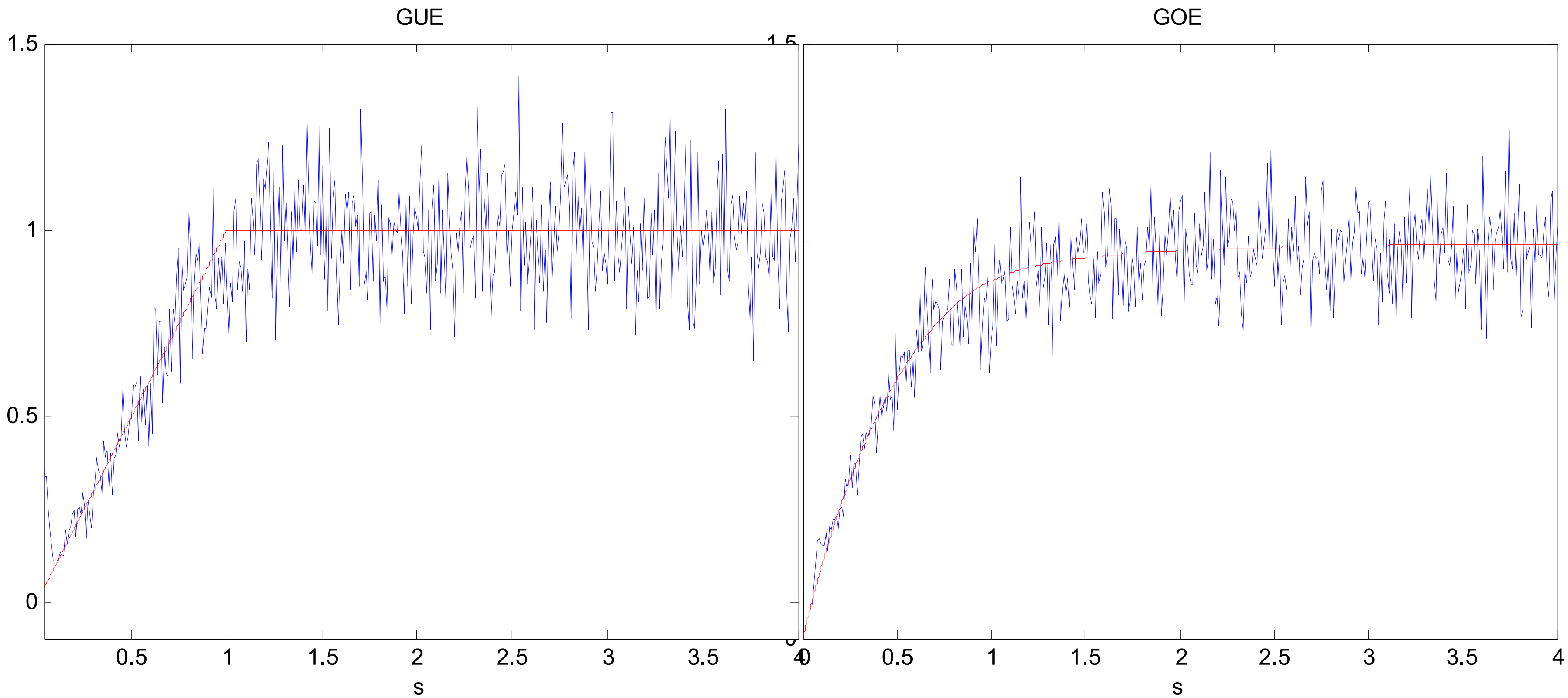

regular graph

The Problem to be addressed:

Why random graphs display the canonical spectral statistics

Counting statistics of cycles *vs* Spectral statistics

The main tool : Trace formulae connecting

spectral information
and
counts of periodic walks on the graph

The periodic walks to be encountered here are special:
Backscattering along the walk is forbidden.
Notation: non-backscattering walks = n.b. walks

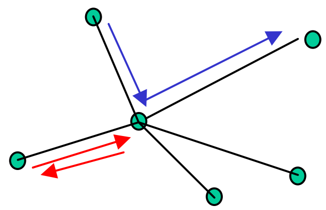

Finite (but large) d-regular graphs in a nut-shell

The R-neighbourhood of every vertex for $R \leq log_{d-1}V$ is almost surely a d-regular tree.

In other words, non-backscattering periodic walks of such period are rare.

Denote by C_t the number of t- cycles (prinitive, non backscatter, non self intersecting t-periodic orbits).

For $t < log_{d-1}V$, the C_t distribute as independent Poisson variables with a mean: $\langle C_t \rangle_{\mathcal{G}} = \frac{(d-1)^t}{2t}$

The Kesten-McKay distribution is derived by computing the spectral density for an infinite d-regular tree and using the local – tree property in the limit of large V.
Note: all the periodic walks on a tree must have at least two backscattering.

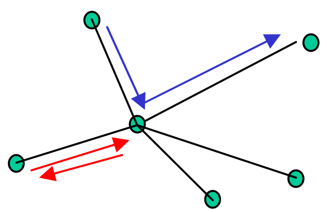

The trace formula:

$$\rho(\lambda) = \frac{d}{2\pi}\frac{\sqrt{4(d-1)-\lambda^2}}{d^2-\lambda^2} + \frac{1}{\pi}\mathcal{R}e\left[\sum_{t=3}^{\infty}\frac{y_t}{\sqrt{4(d-1)-\lambda^2}}\ \mathrm{e}^{it\arccos\frac{\lambda}{2\sqrt{d-1}}}\right]$$

Kesten McKay *Sum over t-periodic non-backscattering walks.*

$$y_t = \frac{1}{V}\frac{[\text{Number of t periodic n.b. walks}] - [(d-1)^t - 1]}{(d-1)^{\frac{t}{2}}}.$$

y_t : The deviation of the number of t-periodic non-backscattering walks from its mean. (properly normalized)

Note: $\langle y_t\rangle_{\mathcal{G}} = 0$ for $t \le \log_{d-1} V$ (Bollobas, McKay, Wormald)

"Action" per single step on the orbit: $\arccos\frac{\lambda}{2\sqrt{d-1}}$

Alternatively:

$$\rho(\lambda) = \frac{d}{2\pi}\frac{\sqrt{4(d-1)-\lambda^2}}{d^2-\lambda^2} + \frac{1}{\pi}\sum_{t=3}^{\infty}\frac{y_t}{\sqrt{4(d-1)-\lambda^2}}\ T_t\left(\frac{\lambda}{2\sqrt{d-1}}\right)$$

$T_l(x)$: Chebyshev Polynomials of the first kind.

Spectral Statistics

The fluctuating part of the spectral densiity :

$$\tilde{\rho}(\lambda) = \rho(\lambda) - \frac{d}{2\pi}\frac{\sqrt{4(d-1)-\lambda^2}}{d^2-\lambda^2} = \frac{1}{\pi}\sum_{t=3}^{\infty}\frac{y_t}{\sqrt{4(d-1)-\lambda^2}}\,T_t\left(\frac{\lambda}{2\sqrt{d-1}}\right)$$

Using the Orthogonality of the Chebyshev Polynomials:

$$y_t = 2\int_{-2\sqrt{d-1}}^{2\sqrt{d-1}} \mathrm{d}\lambda\ \tilde{\rho}(\lambda)\ T_t\left(\frac{\lambda}{2\sqrt{d-1}}\right) = 2\int_{-1}^{1}\mathrm{d}u\ \tilde{\rho}(u)\ T_t(u)$$

$$\langle y_t^2\rangle_{\mathcal{G}} = 4\int_{-1}^{1}\int_{-1}^{1} T_t(u)T_t(v)\ \langle\tilde{\rho}(u)\tilde{\rho}(v)\rangle_{\mathcal{G}}\ dudv$$

Map the spectrum to the unit circle: $\phi = \arccos u\ ,\ \ \phi\in[0,\pi]$

♡ $$\langle y_t^2\rangle_{\mathcal{G}} = 4\int_{0}^{\pi}\int_{0}^{\pi}\cos t\phi\cos t\psi\ \boxed{\langle\tilde{\rho}(\phi)\tilde{\rho}(\psi)\rangle_{\mathcal{G}}}\ d\phi d\psi$$

Two-point correlation function. However:
the spectral variables are not distributed
uniformly and need **unfolding**

♡ $$\langle y_t^2 \rangle_{\mathcal{G}} = 4 \int_0^{\pi} \int_0^{\pi} \cos t\phi \cos t\psi \ \langle \tilde{\rho}(\phi) \tilde{\rho}(\psi) \rangle_{\mathcal{G}} \ d\phi d\psi$$

Define :
$$\widetilde{K}_V(t) \equiv \frac{2}{V-1} \left\langle \left(\sum_{k=1}^{V-1} \cos(t\phi_k) \right)^2 \right\rangle_{\mathcal{G}}$$

The (not unfolded) Spectral formfactor

Therefore
$$\langle y_t^2 \rangle_{\mathcal{G}} = \frac{1}{V} \widetilde{K}_V(t)$$

Spectral form factor = variance of the number of t-periodic nb - walks

Since $\phi \in [0, \pi]$, the mean-spacing is $\frac{2\pi}{2(V-1)}$.

Therefore define $\tau = \frac{t}{2(V-1)}$.

$$C_t = \left\{ \begin{matrix} \text{\# t-periodic} \\ \text{nb orbits} \end{matrix} \right\}$$

For t < logV/log (d-1) C_t are distributed as a Poissonian variable
Hence: variance/mean =1 (Bollobas, Wormald, McKay)

$$\langle y_t^2 \rangle_{\mathcal{G}} = \frac{1}{V} \left\langle \frac{(C_t - \langle C_t \rangle_{\mathcal{G}})^2}{\langle C_t \rangle_{\mathcal{G}}} \right\rangle_{\mathcal{G}} \frac{2t}{V} \xrightarrow[\tau \to 0]{} \frac{1}{V} 2\tau$$

$$\tilde{K}_V(t) = 2\tau \text{ for } \tau \to 0$$

The magnetic adjacency spectral statistics

The non-backtracking magnetic connectivity:

$$Y^{(M)}_{e',e} = \mathrm{e}^{i\phi_{e'}/2}\ B_{e',e}\ \mathrm{e}^{i\phi_e/2}\ - J_{e',e}$$

$$\mathrm{tr}((Y^{(M)})^t) = \sum_{L_t} \mathrm{e}^{i\Phi} + \sum_{R_t} \mathrm{e}^{-i\Phi} + |S_t|$$

L_t = the set of t-periodic nb-walks going clockwise
R_t = the set of t-periodic nb-walks going counter-clockwise
S_t = the set of self-tracing t-periodic nb-walks
These are nb-walks which traverse each edge both ways

$$\langle \mathrm{tr}((Y^{(M)})^t)\rangle_{\mathcal{M}} = |S_t| \ \approx\ 0 \text{ for } \ t < \log_{d-1} V \quad ; \qquad \text{Denote } \langle\cdot\rangle_{\mathcal{G}M} = \langle\cdot\rangle\ .$$

$$\left\langle \left(\mathrm{tr}((Y^{(M)})^t) - \left\langle \mathrm{tr}((Y^{(M)})^t) \right\rangle \right)^2 \right\rangle \approx |L_t| + |R_t| \ \approx\ 2\langle C_t\rangle \cdot t^2$$

$$\approx 4(d-1)^t \left\langle \left(\sum_k \cos(\phi_k) \right)^2 \right\rangle = 8t\langle C_t\rangle \left\langle \left(\sum_k \cos(\phi_k) \right)^2 \right\rangle$$

$$\rightarrow \quad \left\langle \left(\sum_k \cos(\phi_k) \right)^2 \right\rangle \approx \frac{t}{4}$$

By multiplying by $\frac{2}{V-1}$ we get that for short times: $\widetilde{K}(\tau) \approx \tau$.

Going in the reverse direction:
Assuming RMT and computing deviations from the Poisson distribution of t-periodic cycles

$$\widetilde{K}_V(\tau) = \frac{1}{2\pi}\int_0^{2\pi} d\eta K_{RMT}\left(2\tau S^{'}(\eta)\right)$$

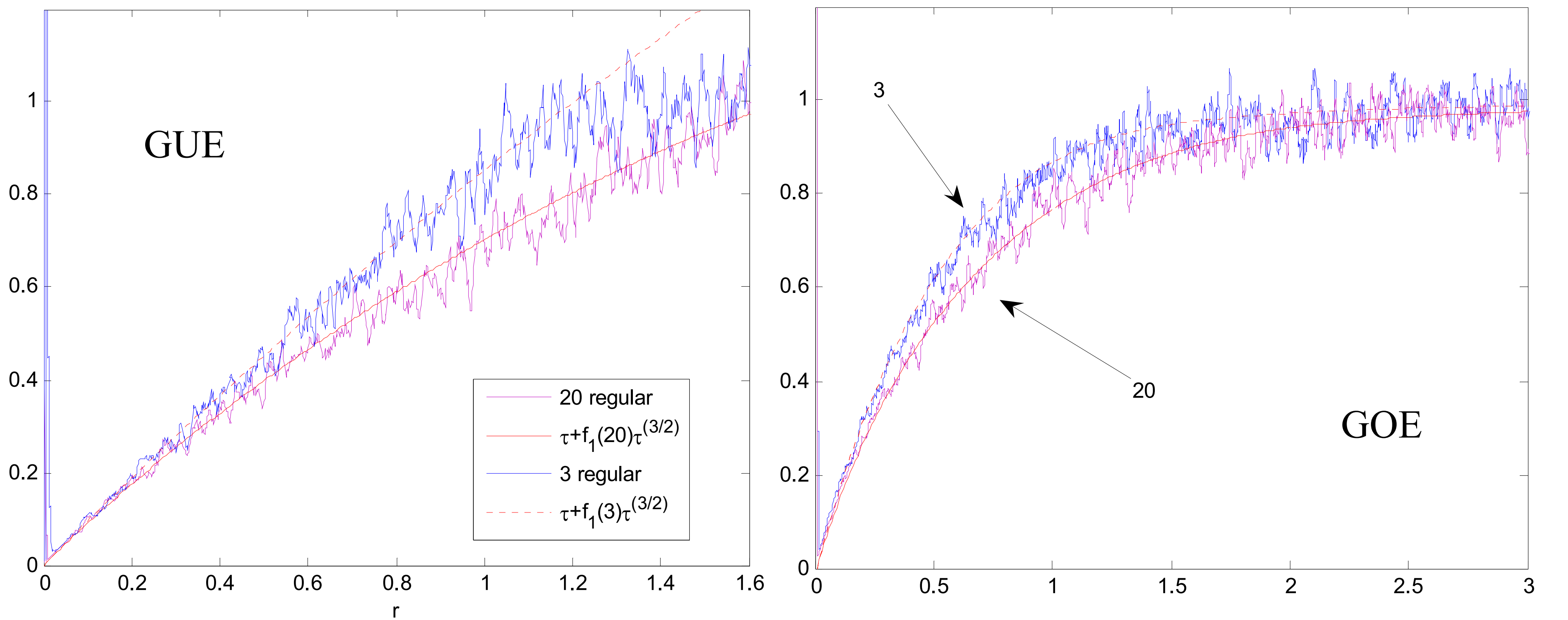

Scaling with d

$$D(d) = \frac{(d-1)^2}{d(d-1)}$$

$$(\widetilde{K}(\tau) - 2\tau) \cdot \frac{\sqrt{D}}{C_O} = \tau^{3/2} + \mathcal{O}(\tau^2)$$

$$(\widetilde{K}(\tau) - \tau) \cdot \frac{\sqrt{D}}{C_U} = \tau^{3/2} + \mathcal{O}(\tau^2)$$

$$C_O = -2\left(1 + \frac{2}{\pi}\left(\frac{\sqrt{2}}{3} - \log\frac{\sqrt{2}+1}{\sqrt{2}-1}\right)\right)$$

$$C_U = -\frac{2\sqrt{2}}{3\pi}$$

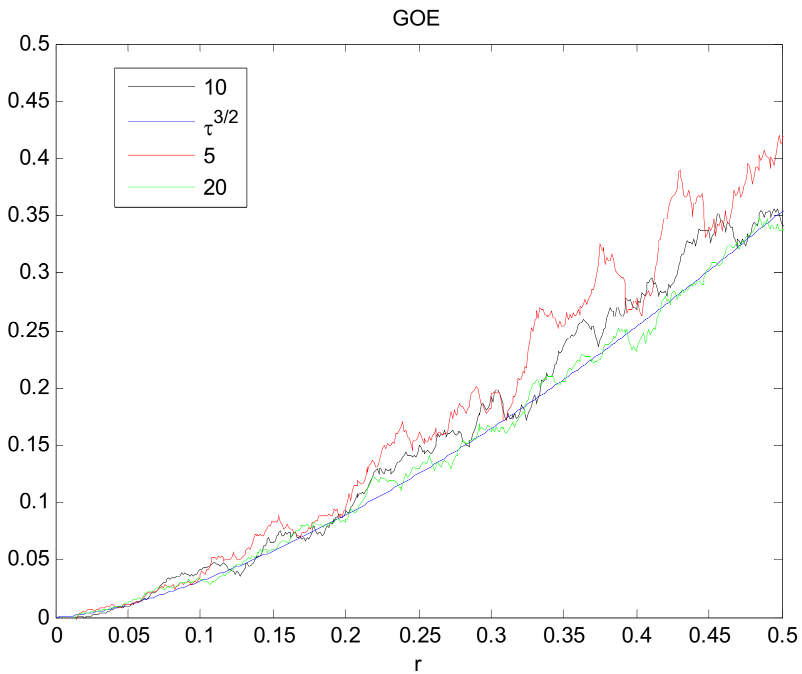

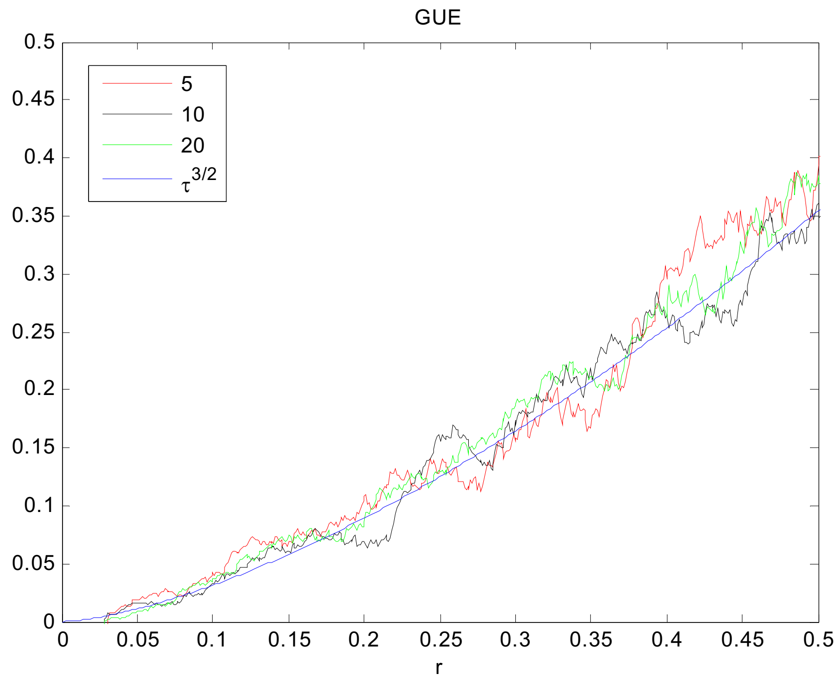

Nodal domains *vs* Percolation on random v-regular graphs

The discrete Laplacian for d-regular graphs:

$$(L\mathbf{f})_i = -\sum_{j\sim i}(f_j - f_i) \;\Rightarrow\; L = -A + d\, I^{(V)}$$

Since L differes from the adjacency matrix A by a constant diagonal matrix, $\Rightarrow$ we study the spectrum of A : $\sigma(\mathcal{G}) = \lambda_0(= d) \geq \lambda_1 \geq, \cdots, \geq \lambda_{V-1}$.

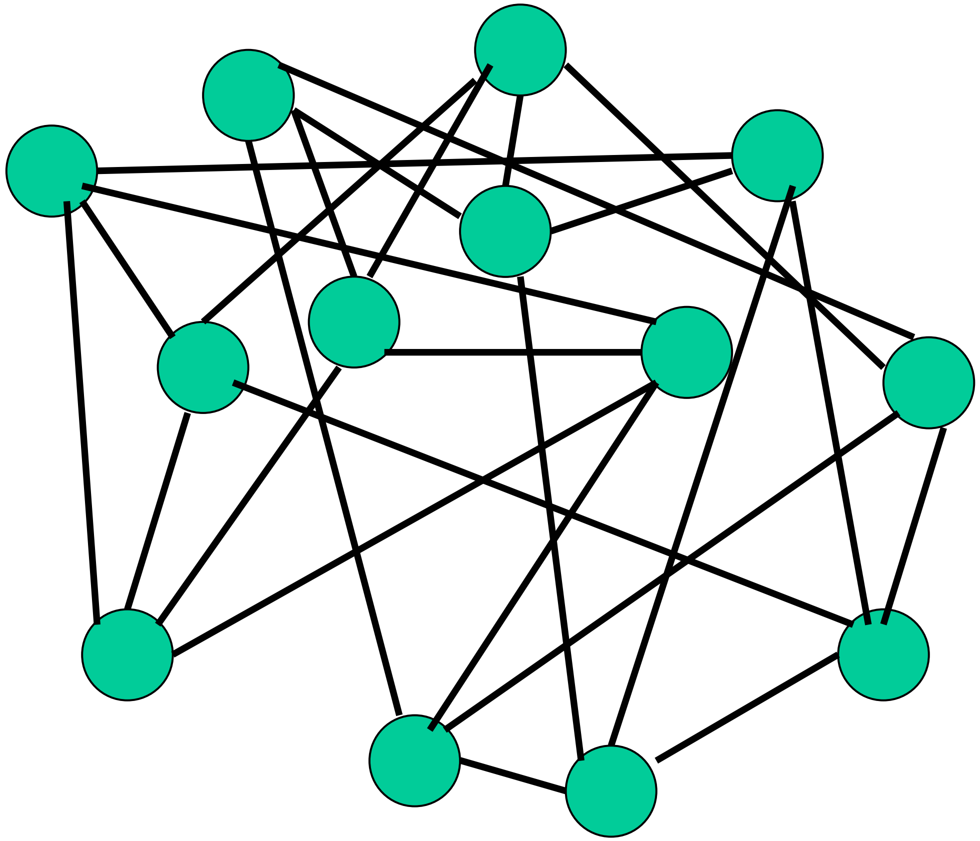

We consider random regular G(V,d) graphs in the limit $V \to \infty$

Percolation on Graphs

(Erdos and Renyi, Alon *et. al.*, Nachmias and Peres)

Start with a random d-regular graph on V vertices.
Perform an independent p-bond percolation :

Retain a bond with a probability p
Delete a bond with a probability $1-p$

Phase transition at $p_c = 1/(d-1)$:

Denote by L the number of vertices in the largest connected component

$p < p_c$	p_c	$p > p_c$
	$\leftarrow 1/V^{1/3} \rightarrow$	
$\boldsymbol{E}(L) \sim o(V^{2/3})$	$\boldsymbol{E}(L) \sim V^{2/3}$	$\boldsymbol{E}(L) \sim o(V^{2/3})\ V^{1/3}$

Bond percolation ~ Vertex percolation

Level sets :

Given an eigenvector **f** *normalized it such that* $-1 < f_i < 1$

For any $0 < p < 1$ *select the sub graph* $\tilde{G}$ *where* $f_i > -1+2p$

Compute the ratio between the cardinality of the largest connected component of the sub-graph $\tilde{G}_{\max}$ *and the cardinality of* $\tilde{G}$.

$|\tilde{G}_{\max}| = 3$

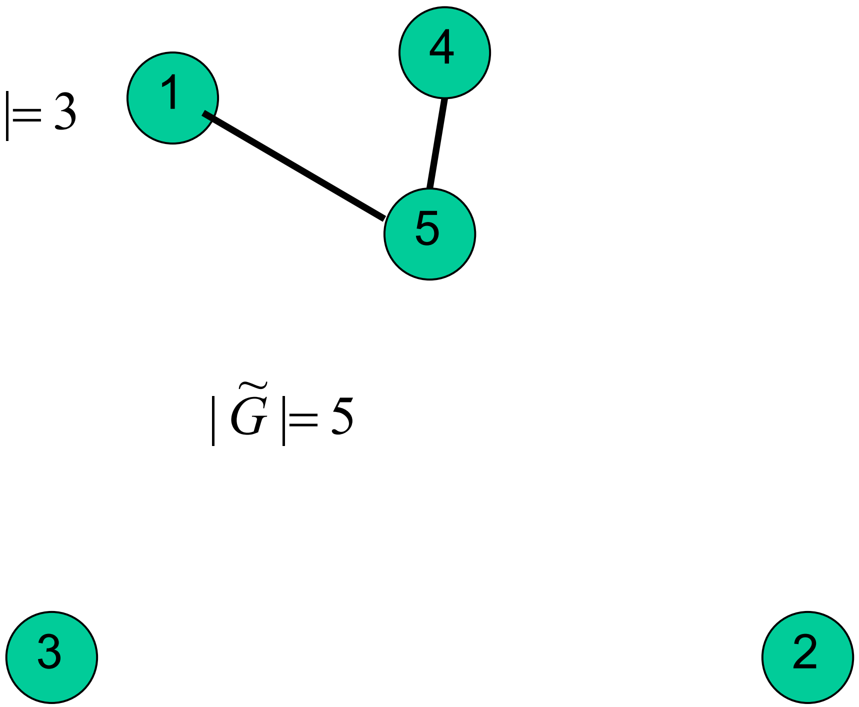

$|\tilde{G}| = 5$

$\tilde{G}$

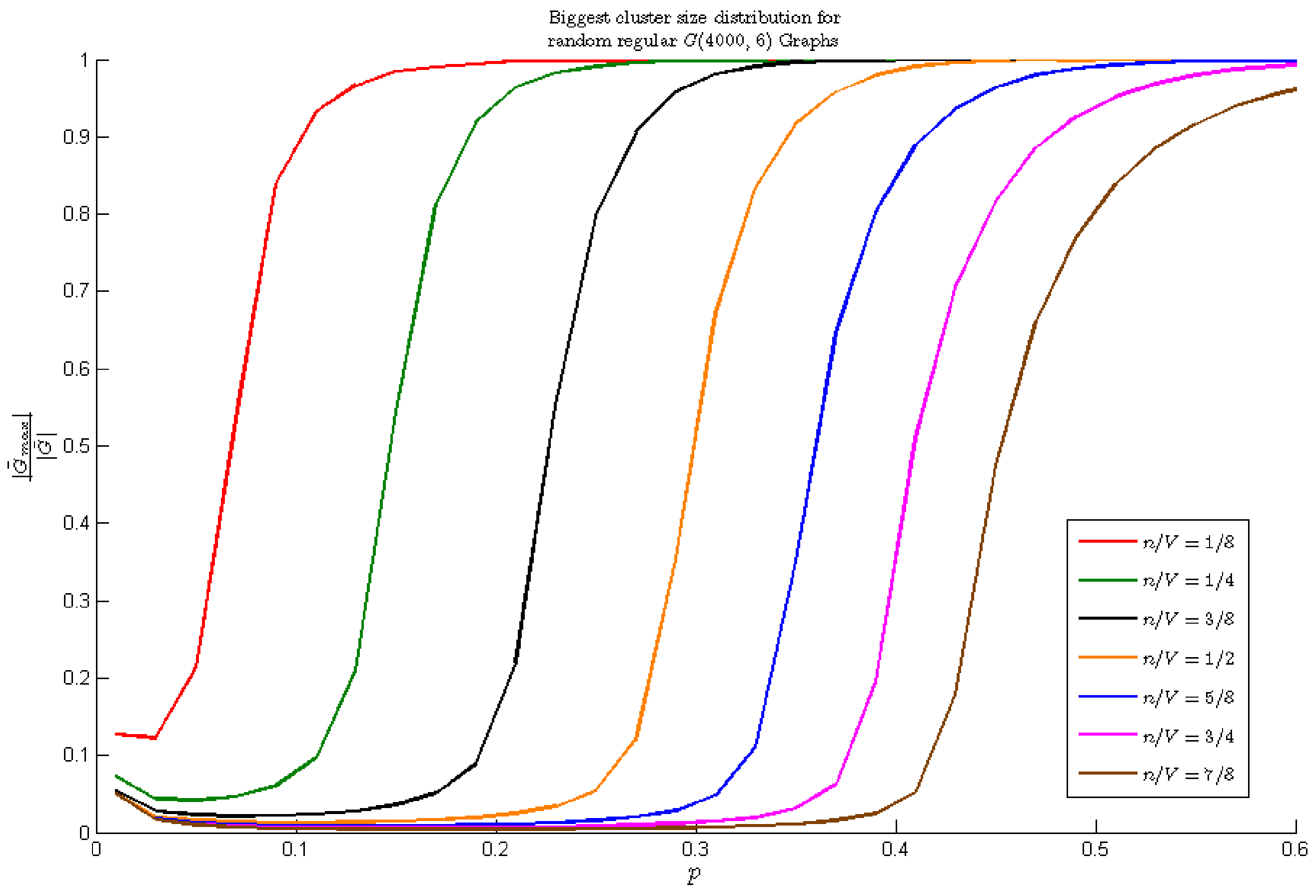

phase transition ?

The shape of the critical surface

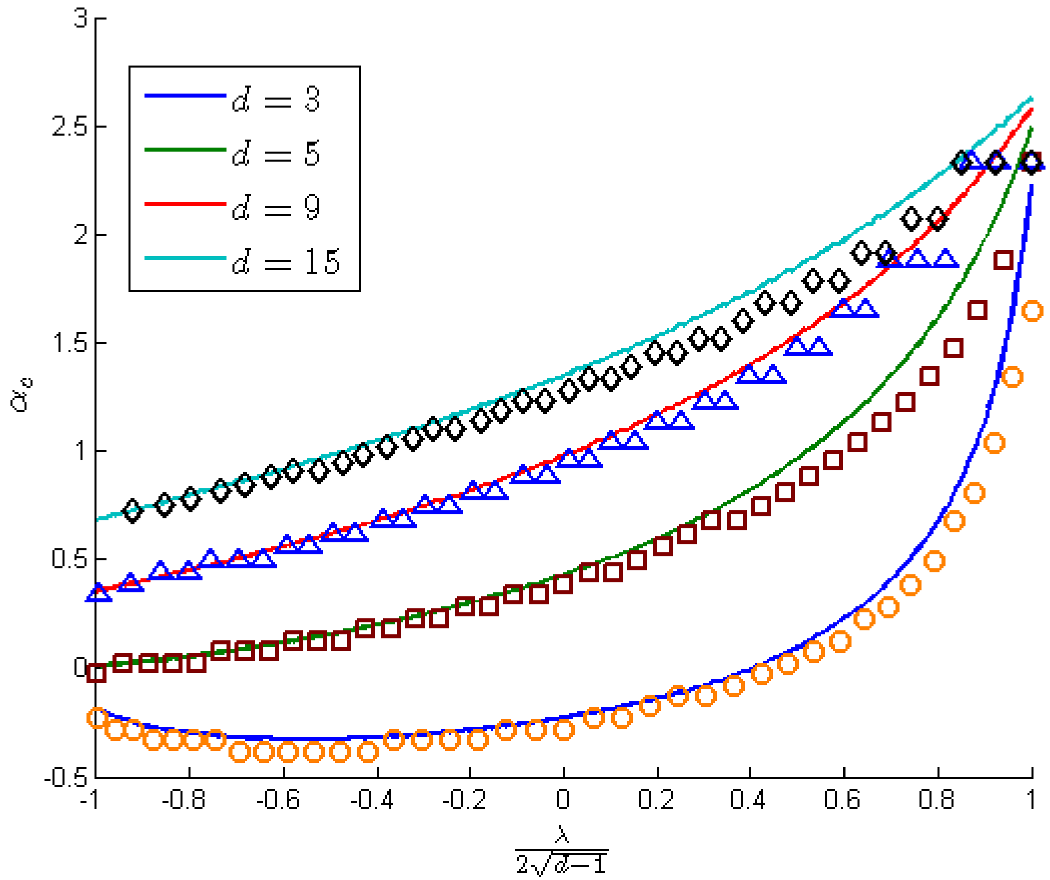

$\alpha_c(\lambda, d)$: the height of the critical level set

Normalization: $\langle f_i^2 \rangle_{\mathcal{G}} = 1$.

"Unpredictability" is the rule and "predictability" is the exception when we observe it in the realm of Quantum Chaos

Yet much information is encoded into the seemingly scrambled Quantum signal

Thank you for your attention